J|A|C|S
ARTICLES

Published on Web 08/02/2010

A Biomimetic Asymmetric Responsive Single Nanochannel

Xu Hou,[‡] Fu Yang,[†,§] Lin Li,[†,§] Yanlin Song,[†] Lei Jiang,*[,†] and Daoben Zhu[†]

Institute of Chemistry, Chinese Academy of Sciences, Beijing 100190, P. R. China, National Center for Nanoscience and Technology, Beijing 100190, P. R. China, and College of Chemistry, Beijing Normal University, Beijing 100875, P. R. China

Received May 25, 2010; E-mail: jianglei@iccas.ac.cn

Abstract: Artificial single nanochannels have emerged as possible candidates for mimicking the process of ionic transport in ion channels and boosting the development of bioinspired intelligent nanomachines for real-world applications, such as biosensors, molecular filtration, and nanofluidic devices. One challenge that remains is to make the artificial nanochannel "smart", with various functions like an organism in Nature. The components of ion channels are asymmetrically distributed between membrane surfaces, which are significant for the implementation of the complex biological function. Inspired by this natural asymmetrical design, here we develop a biomimetic asymmetric responsive single nanochannel system that displays the advanced feature of providing control over pH- and temperature-tunable asymmetric ionic transport properties through asymmetric modifications inside the single nanochannels, which could be considered as a primal platform for the simulation of different ionic transport processes as well as the enhancement of the functionality of ion channels.

Introduction

Living cells depend on ion channels to communicate chemically and electrically with the extracellular environment.[1] The ability to simulate the ionic transport process of ion channels would permit a better understanding of how ion channels work and provide tools for many applications in life science and materials science.[2] One approach is to take an artificial nanochannel[3] of known greater flexibility in terms of shape and size, superior robustness, and surface properties, which can be tuned depending on the desired function, and mimic the biological channels.[4] There has been rapid progress in developing artificial nanochannels that respond to a single external stimulus, such as specific ions,[5] light,[6] pH,[7] temperature,[8] and mechanical stress.[9] However, all of these nanochannels are responsive to only one kind of external stimulus, and endowing these artificial nanochannels with greater intelligence is still a challenging task.[3b,10]

In this work, we further extend the function of biomimetic nanochannel systems by using an asymmetric chemical modification approach.[7f] Compared with previous systems,[5−8] this asymmetric responsive nanochannel system has the advantage that it provides simultaneous control over both the pH- and temperature-tunable asymmetric ionic transport properties. Such a system, as an example, could potentially spark further experimental and theoretical efforts with different complicated functional molecules to exploit more-complex "smart" nanochannel systems.

The shape[11] and chemical properties[12] of the nanochannels are two key factors to control ionic transport properties inside the nanochannels. Once artificial nanochannels are prepared, it

[†] Institute of Chemistry, Chinese Academy of Sciences.
[‡] National Center for Nanoscience and Technology.
[§] Beijing Normal University.

(1) Hille, B. *Ion Channels of Excitable Membranes*; Sinauer Associates: Sunderland, MA, 2001.
(2) (a) Martin, C. R.; Siwy, Z. S. *Science* **2007**, *317*, 331–332. (b) Hou, X.; Jiang, L. *ACS Nano* **2009**, *3*, 3339–3342. (c) Vlassiouk, I.; Apel, P. Y.; Dmitriev, S. N.; Healy, K.; Siwy, Z. S. *Proc. Natl. Acad. Sci. U.S.A.* **2009**, *106*, 21039–21044.
(3) (a) Dekker, C. *Nat. Nanotechnol.* **2007**, *2*, 209. (b) Baker, L. A.; Bird, S. P. *Nat. Nanotechnol.* **2008**, *3*, 73–74.
(4) (a) Jung, Y.; Bayley, H.; Movileanu, L. *J. Am. Chem. Soc.* **2006**, *128*, 15332–15340. (b) Alcaraz, A.; Ramirez, P.; Garcia-Gimenez, E.; Lopez, M. L.; Andrio, A.; Aguilella, V. M. *J. Phys. Chem. B* **2006**, *110*, 21205–21209.
(5) (a) Powell, M. R.; Sullivan, M.; Vlassiouk, I.; Constantin, D.; Sudre, O.; Martens, C. C.; Eisenberg, R. S.; Siwy, Z. S. *Nat. Nanotechnol.* **2008**, *3*, 51–57. (b) Hou, X.; Guo, W.; Xia, F.; Nie, F.-Q.; Dong, H.; Tian, Y.; Wen, L.; Wang, L.; Cao, L.; Yang, Y.; Xue, J.; Song, Y.; Wang, Y.; Liu, D.; Jiang, L. *J. Am. Chem. Soc.* **2009**, *131*, 7800–7805. (c) Tian, Y.; Hou, X.; Wen, L. P.; Guo, W.; Song, Y. L.; Sun, H. Z.; Wang, Y. G.; Jiang, L.; Zhu, D. B. *Chem. Commun.* **2010**, *46*, 1682–1682.
(6) (a) Wang, G. L.; Bohaty, A. K.; Zharov, I.; White, H. S. *J. Am. Chem. Soc.* **2006**, *128*, 13553–13558. (b) Wen, L. P.; Hou, X.; Tian, Y.; Nie, F. Q.; Song, Y. L.; Zhai, J.; Jiang, L. *Adv. Mater.* **2010**, *22*, 1021–1024.
(7) (a) Xia, F.; Guo, W.; Mao, Y. D.; Hou, X.; Xue, J. M.; Xia, H. W.; Wang, L.; Song, Y. L.; Ji, H.; Qi, O. Y.; Wang, Y. G.; Jiang, L. *J. Am. Chem. Soc.* **2008**, *130*, 8345–8350. (b) Yameen, B.; M., A.; Neumann, R.; Ensinger, W.; Knoll, W.; Azzaroni, O. *J. Am. Chem. Soc.* **2009**, *131*, 2070–2071. (c) Ali, M.; Ramirez, P.; Mafe, S.; Neumann, R.; Ensinger, W. *ACS Nano* **2009**, *3*, 603–608. (d) Yameen, B.; Ali, M.; Neumann, R.; Ensinger, W.; Knoll, W.; Azzaroni, O. *Nano Lett.* **2009**, *9*, 2788–2793. (e) Yameen, B.; Ali, M.; Neumann, R.; Ensinger, W.; Knoll, W.; Azzaroni, O. *Chem. Commun.* **2010**, *46*, 1908–1910. (f) Hou, X.; Liu, Y. J.; Dong, H.; Yang, F.; Li, L.; Jiang, L. *Adv. Mater.* **2010**, *22*, 2440–2443.
(8) (a) Yameen, B.; Ali, M.; Neumann, R.; Ensinger, W.; Knoll, W.; Azzaroni, O. *Small* **2009**, *5*, 1287–1291. (b) Guo, W.; Xia, H. W.; Xia, F.; Hou, X.; Cao, L. X.; Wang, L.; Xue, J. M.; Zhang, G. Z.; Song, Y. L.; Zhu, D. B.; Wang, Y. G.; Jiang, L. *ChemPhysChem* **2010**, *11*, 859–864.
(9) Huh, D.; Mills, K. L.; Zhu, X. Y.; Burns, M. A.; Thouless, M. D.; Takayama, S. *Nat. Mater.* **2007**, *6*, 424–428.
(10) Savariar, E. N.; Krishnamoorthy, K.; Thayumanavan, S. *Nat. Nanotechnol.* **2008**, *3*, 112–117.

10.1021/ja1045082

is difficult to change them within a wide range of shape. Therefore, chemical modification of the interior surface of the nanochannels with functional molecules is a critical component in the advancement of smart functional nanochannels, due to the change of sizes and chemical properties of the nanochannels at the narrowest point by ambient stimuli.

In order to achieve different functionalities of the interior surface of artificial nanochannels, various methods have been invented, such as electroless deposition,[13] solution chemical modification,[7a,14] electrostatic self-assembly,[15] and coverage of the whole inner surface of the nanochannels. Recently, we and others have successfully developed temperature-controllable nanochannels with thermally nanoactuated macromolecular gates by electroless deposition and solution chemical modification approaches.[8]

As we know, the components of most biological nanochannels are asymmetrically distributed between membrane surfaces to implement complex biological functions.[16] Inspired by these asymmetrical nanochannels, different asymmetric chemical modification approaches have been developed to enhance the functionality of artificial nanochannels, such as electron beam evaporation,[16] ion sputtering deposition,[18] and plasma modification.[7f,19] Most recently, we have developed a pH-controllable nanochannel which displays the advanced feature of providing simultaneous control over the pH-tunable asymmetric and pH-gated ionic transport properties by using a plasma asymmetric chemical modification approach.[7f] On the basis of our prior work, here we further utilize the specific symmetric shape of a single nanochannel with asymmetric chemical modification approaches to functionalize diverse specific local areas with different functional molecules at nanometer dimensions in order to develop an asymmetric dual-responsive nanochannel system that provides simultaneous control over both the pH- and temperature-tunable asymmetric ionic transport properties. Compared with the single external stimulus systems, the present work is more complicated and moves one step farther toward the development of "smart" nanochannel systems for real-world applications.

As shown in Scheme 1, we prepared a single nanochannel membrane with the well-developed ion track etching technology.[20] The nanochannel was embedded in a track-etched polyethylene terephthalate membrane (PET, Hostaphan RN12 Hoechst, 12 μm thick, with a single ion track in the center). The track-etching technique allows control over the shape of the channels, and in this work the etched single nanochannel is symmetric and hourglass shaped. Diameter measurements of hourglass-shaped nanochannels were conducted with a commonly used electrochemical method.[21] The opening at the base was usually 250−300 nm wide, and the narrow center (tip) was 10−30 nm wide. One side of the nanochannel was treated by plasma-induced grafting in the vapor phase of *N*-isopropylacrylamide (NIPA), which became a temperature-responsive polymer,[22] poly(*N*-isopropylacrylamide) (PNIPA), after plasma-induced graft polymerization (see Supporting Information). The other side of the nanochannel was treated by plasma-induced grafting in the vapor phase of distilled acrylic acid (AAc), which became a pH-responsive polymer,[7f] poly(acrylic acid) (PAA), after plasma-induced graft polymerization. After grafting PNIPA on one side of the hourglass-shaped nanochannel wall and PAA on the other side (center), the PNIPA underwent thermally responsive formation of intermolecular hydrogen-bonding between PNIPA chains and water molecules (left and down) and intramolecular hydrogen-bonding between C═O and N−H groups in PNIPA chains (right and up) below and above the lower critical solution temperature (LCST) of about 32 °C.[23] PAA underwent pH-responsive formation of the intramolecular hydrogen bond among the carboxylic acid groups in the polymer chains (right and down) when the pH was below the pK_a of 4.7 and of the intermolecular hydrogen bonds between PAA chains and water molecules (left and up) when the pH was above the pK_a.[7f,24] These asymmetric temperature/pH-responsive conformational conversions could well induce changes of ionic transport properties inside of the nanochannel and thus realized the asymmetric dual-responsive smart nanochannel system.

The asymmetric responsive ionic transport properties of this nanochannel system were evaluated by measuring the ionic current across the channel in potassium chloride solution (0.1 M). Ionic current measurements were carried out with a Keithley 6487 picoammeter (Keithley Instruments, Cleveland, OH) in a custom-designed electrolyte cell, and the sample membrane was mounted between the two halves of the cell.[5b] Details of single nanochannels preparation, plasma-induced graft polymerization, and current measurement are given in the Experimental Section.

Results and Discussion

Ionic transport properties of the single nanochannel before and after PNIPA/PAA asymmetric chemical modification have been examined by current measurements. Figure 1A shows current−voltage ($I-V$) properties of the nanochannel before chemical modification, and the original nanochannel exhibits linear $I-V$ curves with temperature from 23 to 40 °C at pH 2.8. The degree of ionic rectification was defined as the ratio$_{+/-}$ of absolute values of ionic currents recorded at a given positive voltage (+2 V, anode facing the PNIPA side of the nanochannel) and at the same absolute value of a negative voltage (−2 V, anode facing the PAA side of the nanochannel). Before modification, the ratio$_{+/-}$ (∼1.0) stayed nearly unchanged with temperature from 23 to 40 °C.

After modification, there was an obvious difference, in that the rectifications were observed as asymmetric $I-V$ curves (Figure 1B). By changing the temperature from 23 to 40 °C, the ratio$_{+/-}$ changed from 3.61 ± 0.17 to 1.52 ± 0.03, and the ratio decrease trend coincided with our previous study

(11) Siwy, Z. S.; Howorka, S. *Chem. Soc. Rev.* **2010**, *39*, 1115–1132.
(12) Gyurcsanyi, R. E. *TrAC, Trends Anal. Chem.* **2008**, *27*, 627–639.
(13) Nishizawa, M.; Menon, V. P.; Martin, C. R. *Science* **1995**, *268*, 700–702.
(14) Vlassiouk, I.; Siwy, Z. S. *Nano Lett.* **2007**, *7*, 552–556.
(15) Ali, M.; Yameen, B.; Neumann, R.; Ensinger, W.; Knoll, W.; Azzaroni, O. *J. Am. Chem. Soc.* **2008**, *130*, 16351–16357.
(16) (a) Rothman, J. E.; Lenard, J. *Science* **1977**, *195*, 743–753. (b) Shaw, R. S.; Packard, N.; Schroter, M.; Swinney, H. L. *Proc. Natl. Acad. Sci. U.S.A.* **2007**, *104*, 9580–9584.
(17) Kalman, E. B.; Sudre, O.; Vlassiouk, I.; Siwy, Z. S. *Anal. Bioanal. Chem.* **2009**, *394*, 413–419.
(18) Hou, X.; Dong, H.; Zhu, D. B.; Jiang, L. *Small* **2010**, *6*, 361–365.
(19) Ito, Y.; Park, Y. S. *Polym. Adv. Technol.* **2000**, *11*, 136–144.
(20) (a) Kalman, E. B.; Vlassiouk, I.; Siwy, Z. S. *Adv. Mater.* **2008**, *20*, 293–297. (b) Apel, P. *Radiat. Meas.* **2001**, *34*, 559–566.
(21) Xie, Y. B.; Wang, X. W.; Xue, J. M.; Jin, K.; Chen, L.; Wang, Y. G. *Appl. Phys. Lett.* **2008**, *93*, 163116.
(22) Pan, Y. V.; Wesley, R. A.; Luginbuhl, R.; Denton, D. D.; Ratner, B. D. *Biomacromolecules* **2001**, *2*, 32–36.
(23) Sun, T. L.; Wang, G. J.; Feng, L.; Liu, B. Q.; Ma, Y. M.; Jiang, L.; Zhu, D. B. *Angew. Chem., Int. Ed.* **2004**, *43*, 357–360.
(24) Lee, J. W.; Kim, S. Y.; Kim, S. S.; Lee, Y. M.; Lee, K. H.; Kim, S. J. *J. Appl. Polym. Sci.* **1999**, *73*, 113.

Scheme 1. Biomimetic Asymmetric Responsive Single Nanochannel System[a]

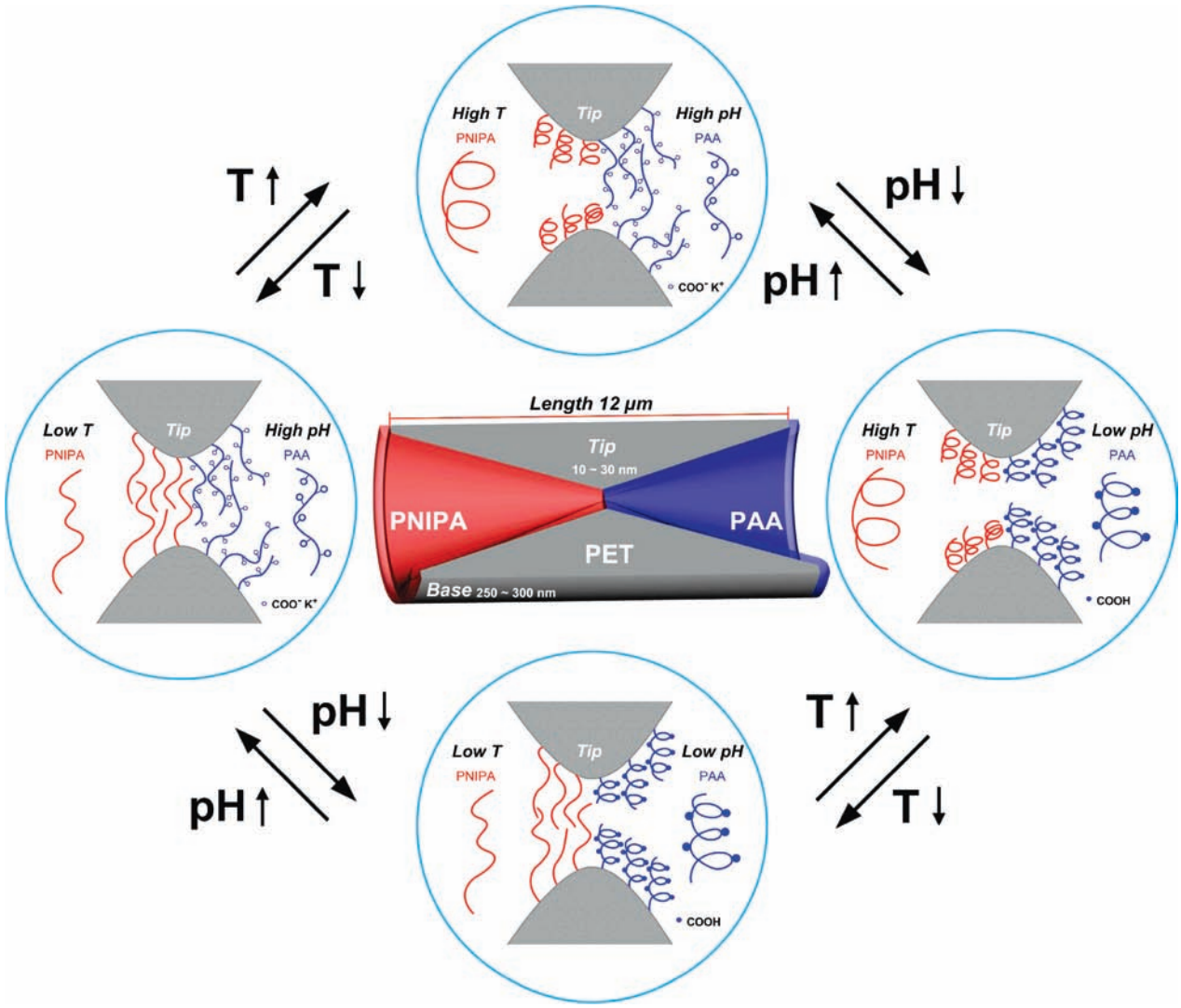

[a] After asymmetric chemical modification of a single hourglass-shaped nanochannel (center), PNIPA was immobilized on one side of the inner surface of the single nanochannel, and PAA was immobilized on the other side. When the temperature changed within a certain range, PNIPA underwent thermally responsive formation of intermolecular hydrogen-bonding between PNIPA chains and water molecules (left and down) and intramolecular hydrogen-bonding between C═O and N−H groups in PNIPA chains (right and up) below and above LCST. At the same time, when the pH changed within a certain range, PAA underwent pH-responsive formation of the intramolecular hydrogen bond among the carboxylic acid groups in the polymer chains (right and down) when the pH was below the pK_a and of the intermolecular hydrogen bonds between PAA chains and water molecules (left and up) when the pH was above the pK_a. Before modification, the etched hourglass-shaped single nanochannels are 10−30 nm wide at the narrowest point. (Drawing not to scale.)

on the temperature responsive single funnel-shaped metal−polymer composite nanochannel.[8b] It is worth mentioning that there was a remarkable asymmetric ionic current increase when the temperature was changed from 23 to 32 °C, compared with changing the temperature from 32 to 40 °C. This behavior can be explained by the mechanism shown in Figure 1C.

It is generally believed that PNIPA maintains a swollen state at 23 °C and exhibits a thermally responsive transition into a collapsed state below and above LCST of about 32 °C.[23] Raising the temperature from 23 to 32 °C promotes drastic changes in the conformational state of the PNIPA. In this case, there is an obvious increase of the effective pore size of the nanochannel, which is evidenced as a larger increase in ionic current. On continuing to raise the temperature from 32 to 40 °C, the conformational state of the PNIPA stayed nearly unchanged. In this case, there is no increase of the effective pore size of the nanochannel, and the ionic current increase coming from the conductivity changes due to temperature variations, the same as ionic transport properties of the original nanochannel. It is clear that that asymmetric ionic transport property was caused by the asymmetric PNIPA modification, which gives structural asymmetry and nonuniform chemical composition to the nanochannel. This nanochannel system has the advantage that it provides simultaneous thermally controllable and asymmetric ionic transport properties that the other temperature-responsive nanochannels[8a] do not have.

Figure 2A shows $I-V$ properties of the nanochannel before chemical modification, and the original nanochannel exhibits linear $I-V$ curves with pH from 2.8 to 10 at 23 °C. The ratio$_{+/-}$ (∼1.0) stayed nearly unchanged with pH from 2.8 to 10, which meant that the original nanochannel does not rectify at different pH values. After modification, there was a remarkable difference: a significant increase in the transmembrane ionic current could be observed when the pH

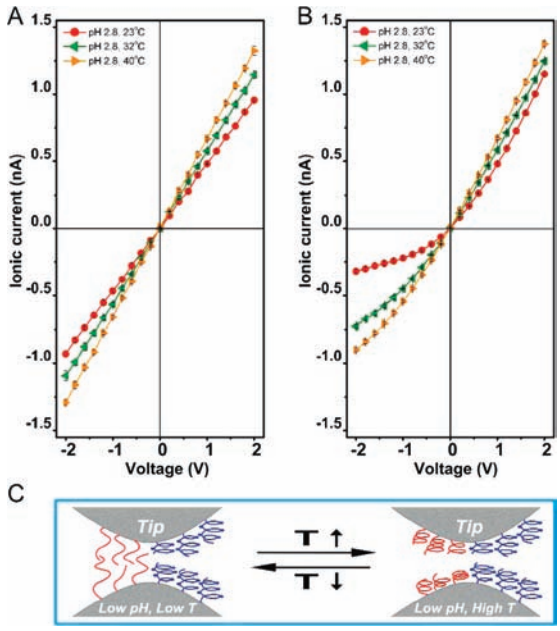

Figure 1. Current−voltage ($I-V$) properties of the single nanochannel (A) before and (B) after PNIPA was attached onto one side of the inner channel wall and PAA was attached onto the other side (asymmetric chemical modification). $I-V$ characteristics were recorded under symmetric electrolyte conditions (pH 2.8) at 23 (red circles), 32 (green triangles), and 40 °C (orange triangles). (C) Explanation of the asymmetric dual-responsive ionic transport properties of this single hourglass-shaped nanochannel system at low pH with different temperatures. (Sample: base ∼290 nm, tip ∼18 nm, before chemical modification.)

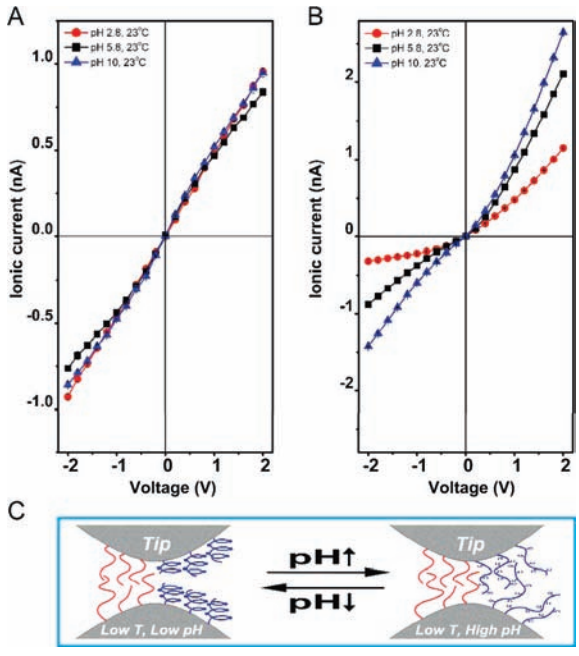

Figure 2. $I-V$ properties of the single nanochannel (A) before and (B) after asymmetric chemical modification. $I-V$ characteristics were recorded under symmetric electrolyte conditions (23 °C) at pH 2.8 (red circles), 5.8 (black squares), and 10 (blue triangles). (C) Explanation of the asymmetric dual-responsive ionic transport properties of this single hourglass-shaped nanochannel system at low temperature with different pH values.

changed from 2.8 to 10 in Figure 2B. By changing the pH from 2.8 to 10, the ratio$_{+/-}$ changed from 3.6 ± 0.17 to 1.86 ± 0.01. According to our previous pH-controllable nanochannel work,[7f] it was thought that this pH-responsive ionic

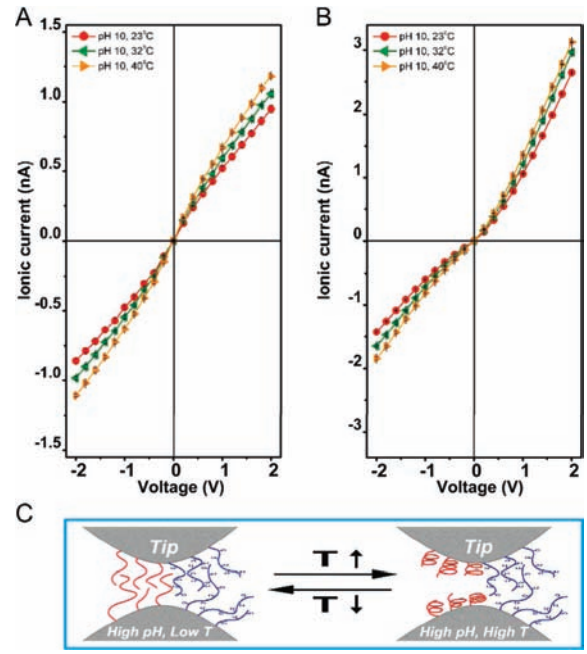

Figure 3. $I-V$ properties of the single nanochannel (A) before and (B) after asymmetric chemical modification. $I-V$ characteristics were recorded under symmetric electrolyte conditions (pH 10) at 23 (red circles), 32 (green triangles), and 40 °C (orange triangles). (C) Explanation of the asymmetric dual-responsive ionic transport properties of this single hourglass-shaped nanochannel system at high pH with different temperatures.

transport property was caused by asymmetric PAA modification, and the pH-responsive capabilities can be controlled, depending on the size of the original nanochannel and the degree of plasma modification. It was assumed that during the pH changes from low to high, the wettability of the channel plays a prominent role in the ionic transport properties because of the PAA transition from a hydrophobic state to a hydrophilic state. This behavior can be explained by the mechanism shown in Figure 2C.

It was assumed that the effective pore size of the nanochannel was determined by two aspects in this system, that is, the changes of physical block and charge density by the molecular conformational change.[5b] In our system, the physical block and charge density would change simultaneously because the PAA molecules were negatively charged above pK_a. Thus, these two factors were integrated to investigate the "effective pore size" change, which could more comprehensively explain the phenomenon in our asymmetric responsive system.

Raising the temperature, compared with PAA, the conformation of the PNIPA chains changes from the swollen state to the collapsed state, and there is also a conformational transition that changes the wettability of the nanochannel. The PNIPA transition, in contrast, is from a hydrophilic state to a hydrophobic state. The phenomenon of the responsive properties of the nanochannel is explained by the competition between two factors, that is, the changes of the effective pore size and the wettability. It is reasonable that when PNIPA transitions from the swollen state to the collapsed state, the effective pore size and the wettability of the nanochannel change at the same time. PNIPA neutralized the surface charge of the nanochannel, resulting in asymmetric surface charge of the inner surface of the symmetric nanochannel, and the increase of the effective pore size of nanochannel

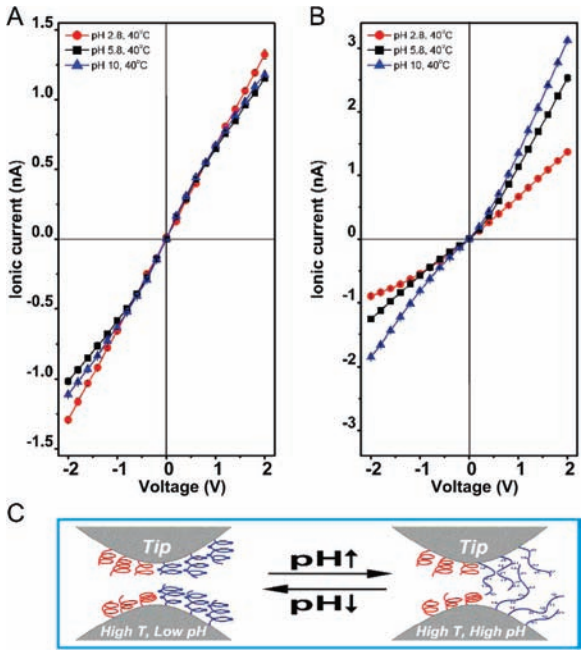

Figure 4. $I-V$ properties of the single nanochannel (A) before and (B) after asymmetric chemical modification. $I-V$ characteristics were recorded under symmetric electrolyte conditions (40 °C) at pH 2.8 (red circles), 5.8 (black squares), and 10 (blue triangles). (C) Explanation of the asymmetric dual-responsive ionic transport properties of this single hourglass-shaped nanochannel system at high temperature with different pH.

played a prominent role in ionic transport properties. It is worth mentioning that the pH-responsive PAA molecules have negatively charged carboxyl groups. When the pH is above the pK_a, PAA molecules were highly negatively charged. This property might effectively reduced the decrease of the effective pore size of the nanochannel during the change in the conformation of the PAA chains from coiled to stretch, due to mutual electrostatic repulsion between PAA charged molecules. In our case, it is clear that PNIPA and PAA would change simultaneously, and the pH responsivity is, of course, greater than the temperature responsivity.

Figure 3A shows $I-V$ properties of the nanochannel before chemical modification, and the ratio$_{+/-}$ (∼1.1) stayed nearly unchanged with temperature from 23 to 40 °C. After modification, the $I-V$ curves were asymmetric (Figure 3B), and the ratio$_{+/-}$ changed from 1.86 ± 0.01 to 1.70 ± 0.02 upon changing the temperature from 23 to 40 °C. As mentioned above, the influence of pH is greater than that of temperature. Although the effective pore size increased during the temperature increase at high pH, that phenomena was not obseerved at the low pH state: the ratio change is obvious, and the asymmetric ionic current increases with temperature from 23 to 32 °C. This behavior can be explained by the mechanism shown in Figure 3C.

Figure 4A shows $I-V$ properties of the original nanochannel, which exhibits linear $I-V$ curves with pH from 2.8 to 10 at 40 °C. The ratio$_{+/-}$ (∼1.0) stayed nearly unchanged with pH from 2.8 to 10. Compared to the low-temperature state, the nanochannel after modification showed a similar increasing trend with pH from 2.8 to 10, which was also observed as asymmetric $I-V$ curves (Figure 4B). However, the ratio$_{+/-}$ significantly decreases with the increasing temperature from 23 to 40 °C. As mentioned above, there is an obvious increase of the effective pore size of the nanochannel upon changing the temperature from 23 to 40 °C, and it is generally believed that the ionic rectification decreases with the increase of the nanometer dimensions of the effective pore size induced by ambient stimuli.[25] This behavior can be explained by the mechanism shown in Figures 2C and 4C.

As shown in Figure 5A, the ionic current in the nanochannel before modification stayed nearly unchanged by different temperature and pH, which meant that the original nanochannel does not rectify. In our smart nanochannel system, there is a negative correlation between the ratio$_{+/-}$ and the temperature at various pH values (Figure 5B). This property could be attributed to the thermally responsive PNIPA transition from the swollen state to the collapsed state, which induced the change of the effective pore size of the nanochannel. In addition, at low pH state, the change of this negative correlation is remarkable. It can be concluded that when the pH is below the pK_a, PAA molecules were uncharged, the contribution of PAA for ionic transport properties was largely reduced, and the contribution of PNIPA response played a prominent role in asymmetric ionic transport properties of the nanochannel by asymmetric adjustment of the effective pore size, whereas when the pH was above the pK_a, PAA molecules were highly negatively charged and the contribution of PAA started to exert a main influence on the ionic transport properties of the nanochannel.

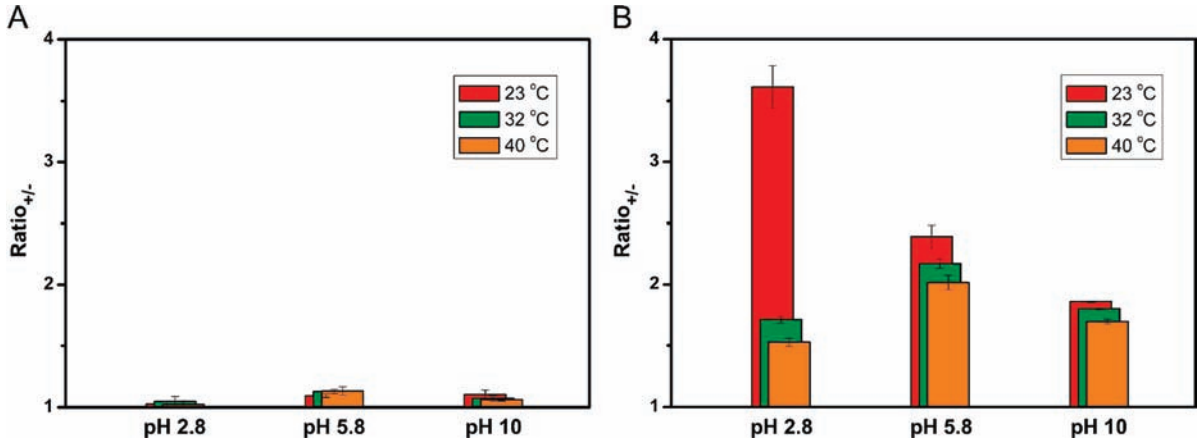

Figure 5. Ionic current rectification of the single nanochannel (A) before and (B) after asymmetric chemical modification (23 °C, red; 32 °C, green; 40 °C, orange) at 2 V.

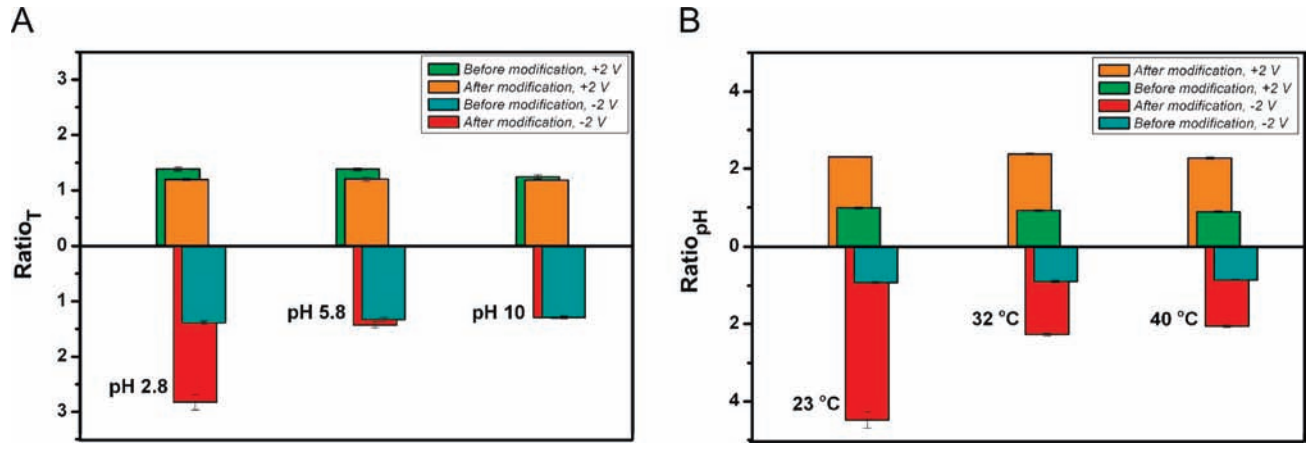

Figure 6. Asymmetric responsive ionic transport properties of the nanochannel. (A) Current ratio of a high-temperature (40 °C) state versus a low-temperature (23 °C) state calculated in the single nanochannel before (green and cyan) and after (orange and red) asymmetric chemical modification with positive potential +2 V (anode facing the PNIPA side of the nanochannel, above) and negative potential −2 V (anode facing the PAA side of the nanochannel, below). (B) Current ratio of pH 10 state versus pH 2.8 state calculated in the single nanochannel before (green and cyan) and after (orange and red) asymmetric chemical modification with positive potential +2 V (above) and negative potential −2 V (below).

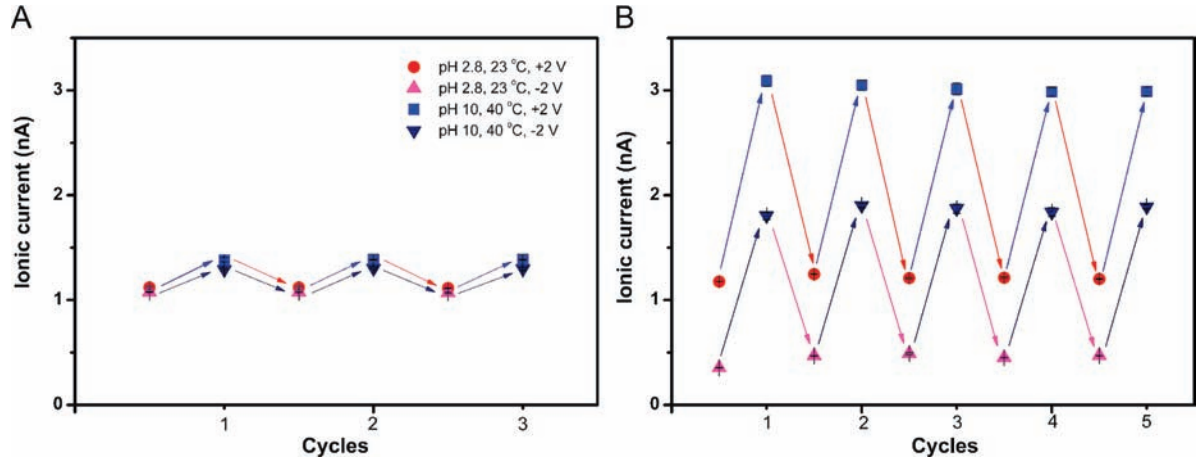

Figure 7. Stability and responsive switching ability of the nanochannel. Reversible variation of the ionic current transport of the single nanochannel before (A) and after (B) asymmetric chemical modification at +2 V (pH 2.8 and 23 °C, red circles; pH 10 and 40 °C, blue squares) and −2 V (pH 2.8 and 23 °C, magenta triangles; pH 10 and 40 °C, navy triangles).

To explore the asymmetric temperature-responsive properties with various pH, the degree of temperature influence on ionic transport properties of the nanochannel was defined as the ratio$_T$ of values of ionic currents recorded at a high temperature state (40 °C) as T_{high} and a low temperature state (23 °C) as T_{low}. As shown in Figure 6A, the ratio$_T$ of values of the original nanochannel stayed around 1.3 at ±2 V with pH from 2.8 to 10. After modification, the ratio$_T$ of values of the nanochannel was around 1.2 at +2 V, and from 2.83 ± 0.14 to 1.29 ± 0.01 at −2 V. This result again verified that the asymmetric responsive ionic transport property was caused by asymmetric chemical modification and the temperature-responsive capabilities reduced by increasing the pH.

Figure 6B shows the asymmetric pH-responsive properties with various temperature. The degree of pH influence on ionic transport properties of the nanochannel was defined as the ratio$_{pH}$ of values of ionic currents recorded at a high pH state (pH 10) as base and a low pH state (pH 2.8) as acid. The ratio$_{pH}$ of values of the original nanochannel stayed around 0.9 at ±2 V with temperature from 23 to 40 °C. After modification, the ratio$_T$ of values of the nanochannel was around 2.3 at +2 V, and from 4.48 ± 0.21 to 2.05 ± 0.04 at −2 V. It is clear that the pH-responsive capabilities were also reduced by increasing the temperature.

To determine the stability and the responsive switching ability of the nanochannel, further studies have been done and are shown in Figure 7. The time scale of each cycle of the responsive switching experiment is about 30 min, due to the temperature control and stability. There is a stability of the original symmetric nanochannel (Figure 7A), which is an ideal platform for developing smart nanochannel systems. The responsive switching ability of the smart nanochannel system upon alternating both the pH and the temperature of the test solution is shown in Figure 7B, which reflects the reproducible and reversible character of the asymmetric responsive nanochannel.

Conclusions

In summary, we experimentally demonstrate a biomimetic asymmetric responsive single nanochannel system, which displays the advanced feature of providing simultaneous control over both pH- and temperature-tunable asymmetric ionic transport properties. The responsive properties of the smart nanochannel are explained by the competition between

(25) Siwy, Z. S. *Adv. Funct. Mater.* **2006**, *16*, 735–746.

two factors: the changes of the effective pore size and the wettability. Increasing the temperature or the pH reduces the asymmetric responsive capabilities. We believe that this asymmetric system can be extended to higher levels of functionality through designing more complicated functional molecules. This novel system is as an example of the beginning of multiresponsive nanochannel systems and moves one step farther toward the development of "smart" nanochannel systems for real-world applications.[26]

Experimental Section

Nanochannels Preparation. The single hourglass-shaped nanochannel was produced in PET polymer film using the well-developed ion track-etching technique. Before the chemical etching process, the samples of the polyethylene terephthalate membrane (PET, Hostaphan RN12 Hoechst, 12 μm thick, with single ion track in the center) were exposed to the UV light for 1 h from each side. To produce an hourglass-shaped nanochannel, etching was performed from both sides. For the observation etching process, the voltage (1 V) used to monitor the etching process was applied in such a way that the transmembrane ionic current can be observed as soon as the nanochannel opened. To both sides of the cell were added a solution that is able to neutralize the etchant as soon as the nanochannel opens, thus slowing down the further etching process. The following are the etching and stopping solutions for the etching of PET: 9 M NaOH for etching, 1 M KCl + 1 M HCOOH for stopping. The opening of the hourglass-shaped nanochannel was called the base, while the small center was called the tip. The diameter of the base was estimated from the multitrack membranes etch rate measured in the parallel etching experiments by environmental scanning electronic microscopy. In this work, the base of the single channel is usually controlled from ~250 to ~300 nm, and its tip is from ~10 to ~30 nm.

Plasma-Induced Graft Polymerization. The PET film should first be soaked in water for 5 h after the etching experiment. There are two steps for our asymmetric chemical modification approach. First step, one side of the nanochannel was modified with PNIPA. NIPA was placed in a monomer delivery system (Suzhou Omega Machinery Electronic Technology Co., Ltd., DJ-02). Vacuum before switching on the glow discharge was 5 Pa, and the working temperature was maintained at 92 °C, due to the low of volatility of NIPA. In our experiment setup, the loop of pumping and releasing argon gas in the reaction chamber (Suzhou Omega Machinery Electronic Technology Co., Ltd., DT-02) runs three times. NIPA monomers were then transported to the reaction chamber, and it was maintained at a power of 20 W to glow discharge in the reaction chamber. At the same time, the argon atmosphere was kept about 40−60 Pa, and this process lasted for 15 min. After the glow extinguished, it continued for about 20 min under vacuum of 40−60 Pa for the grafting reaction. After that, the chamber was connected with air. For the second step, the other side of the nanochannel was modified with PAA. Distilled AAc was injected into plasma induced grafting reactor (Suzhou Omega Machinery Electronic Technology Co., Ltd., DJ-01). Vacuum before switching on the glow discharge was 21 Pa, and the working temperature was 20 °C. In our experiment setup, the argon atmosphere was kept about 50−70 Pa, and the process lasted for 15 min. It continued about 10 min for Start R-F power supply source (Suzhou Omega Machinery Electronic Technology Co., Ltd., DT-01) at 20 W to glow discharge. After the glow extinguished, the grafting reactor would lead to grafting AAc monomers, maintaining the vacuum at 150−300 Pa. The grafting reaction lasted about 20 min. After that, the chamber was connected with air. The plasma treatment was finished. At present, the experimental results of the asymmetric responsive ionic transport properties of our channel system as the indirect evidence favor the asymmetric chemical modification.

Current Measurement. The ionic transport properties of the nanochannel were studied by measuring ionic current through the nanochannels before and after plasma treatment. Ionic current was measured by a Keithley 6487 picoammeter (Keithley Instruments, Cleveland, OH). A single hourglass-shaped PET membrane was mounted between two chambers of the etching cell mentioned above. Ag/AgCl electrodes were used to apply a transmembrane potential across the film. Forward voltage was the potential applied on one of base sides, which is the PNIPA side of the nanochannel. The main transmembrane potential used in this work was evaluated, and a scanning voltage varied from −2 to +2 V with a 40 s period was selected. The pH of the electrolyte was adjusted by 1 M HCl and KOH solutions, and the influence of addition substance quality can be ignored. It should be clear that all the pH values in this work are mensurated at 20 °C. All measurements were carried out in a custom-designed temperature control system. In this work, each test was repeated five times to obtain the average current value at different voltages on the same channel.

Acknowledgment. We thank the Material Science Group of GSI (Darmstadt, Germany) for providing the ion-irradiated samples. This work was supported by the National Research Fund for Fundamental Key Projects (2010CB934700, 2009CB930404, 2007CB936403, 2007CB936400) and National Natural Science Foundation (20974113, 20920102036). The Chinese Academy of Sciences and National Center for Nanoscience and Technology are gratefully acknowledged. We also thank Dr. L. Chen, H. Dong (Institute of Chemistry, Chinese Academy of Sciences), and Dr. H. W. Wang (Suzhou Omega Machinery Electronic Technology Co. Ltd.) for beneficial discussions.

Supporting Information Available: XPS test of PET films before and after PNIPA modification and complete ref 26e. This material is available free of charge via the Internet at http://pubs.acs.org.

JA1045082

(26) (a) Xia, F.; Jiang, L. *Adv. Mater.* **2008**, *20*, 2842–2858. (b) Griffiths, *J. Anal. Chem.* **2008**, *80*, 23–27. (c) Kasianowicz, J. J.; Brandin, E.; Branton, D.; Deamer, D. W. *Proc. Natl. Acad. Sci. U.S.A.* **1996**, *93*, 13770–13773. (d) Sowerby, S. J.; Broom, M. F.; Petersen, G. B. *Sens. Actuators B* **2007**, *123*, 325–330. (e) Branton, D.; et al. *Nat. Biotechnol.* **2008**, *26*, 1146–1153.